

Extracting the Green's function from the correlation of coda waves: A derivation based on stationary phase

Roel Snieder

Center for Wave Phenomena and Department of Geophysics, Colorado School of Mines, Golden, Colorado 80401-1887, USA

(Received 30 May 2003; revised manuscript received 2 December 2003; published 29 April 2004)

The Green's function of waves that propagate between two receivers can be found by cross-correlating multiply scattered waves recorded at these receivers. This technique obviates the need for a source at one of these locations, and is therefore called "passive imaging." This principle has been explained by assuming that the normal modes of the system are uncorrelated and that all carry the same amount of energy (equipartitioning). Here I present an alternative derivation of passive imaging of the ballistic wave that is not based on normal modes. The derivation is valid for scalar waves in three dimensions, and for elastic surface waves. Passive imaging of the ballistic wave is based on the destructive interference of waves radiated from scatterers away from the receiver line, and the constructive interference of waves radiated from secondary sources near the receiver line. The derivation presented here shows that the global requirement of the equipartitioning of normal modes can be relaxed to the local requirement that the scattered waves propagate on average isotropically near the receivers.

DOI: 10.1103/PhysRevE.69.046610

PACS number(s): 43.20.+g, 91.30.-f, 42.30.-d

I. INTRODUCTION

Passive imaging is a technique wherein waves recorded at two receiver locations are correlated to give the Green's function that describes the direct wave propagation between these receivers. The tail of multiply scattered waves is called the "coda," after the Latin word for tail. Coda waves are effective for monitoring temporal changes in media [1,2]. Using coda waves to determine the Green's function is useful because it provides information on wave propagation between two points in space without the need for a source at either of these two points. The Green's function thus obtained can be used to form an image of the medium. Passive imaging has been used in seismic exploration [3,4], helioseismology [5], and ultrasonics with either an active source [6–8] or thermal noise that excites the coda [9,10]. Numerical experiments have shown that passive imaging can be used both in closed and in open systems [11,12].

Campillo and Paul [13] recently used passive imaging in crustal seismology by retrieving the surface wave Green's function between seismological stations within Mexico using coda waves generated by earthquakes along the west coast of Mexico. The theoretical explanation offered in their work is based on the assumption of equipartitioning of the Earth's modes [6]. These modes can either be the normal modes of the Earth, or the surface wave modes that describe the guided waves that propagate along the Earth's surface.

Suppose one invokes the Earth's normal modes. In the study of Campillo and Paul [13], records of the ground motion with a duration of about 600 s were used. It takes about 1100 s for a P wave to propagate to the other side of the Earth [14]; for an S wave it takes even longer, so, in their study, the time is too short for the Earth's normal modes to equilibrate. Invoking the surface wave modes, however, also poses a conceptual problem. These modes are guided waves, and they are not discrete because they exist for every frequency. (For any given frequency there is a discrete set of

allowable wave numbers [15,16].) Furthermore, because of the shallow depth of most earthquakes, the fundamental Love and Rayleigh wave modes are usually most strongly excited and, in regional seismology, there is no equipartitioning of energy among surface wave modes because the fundamental Love and Rayleigh wave modes usually carry more energy than the sum of all higher modes [17,18]. This means that both the Earth's normal modes as well as the surface wave modes cannot be used to explain the experiments of Campillo and Paul [13]. This does not mean that the derivation of passive imaging based on normal modes [6] is incorrect, but it does imply that it is not always applicable.

The goal of this work is to present an alternative way to understand why the correlations hidden in the coda provide the ballistic wave Green's function between the receivers. In Sec. II, I illustrate this with the simplest case of scalar waves in a homogeneous medium having embedded scatterers. In Sec. III, the results are interpreted and the role of the scattering medium is elucidated. In Sec. IV, I extend the derivation to elastic surface waves in three dimensions (3D). The derivation presented here is not based on normal modes; therefore, it is valid both for closed and open systems.

II. PASSIVE IMAGING FOR SCALAR WAVES IN A 3D MEDIUM

Consider two receivers that are separated by a distance R , as shown in Fig. 1. I use a coordinate system with the origin chosen at receiver 1 and with the positive x axis in the direction of receiver 2. The receivers are placed in a medium with scatterers s that radiate scalar waves. Apart from the scatterers, the propagation velocity is assumed to be constant. The scatterers act as secondary sources of singly and multiply scattered waves; scatterer number s emits a signal $S_s(t)$ that is due to all the waves that impinge upon that scatterer. The wave field at the two receivers can be written as a superposition of the waves radiated by the scatterers

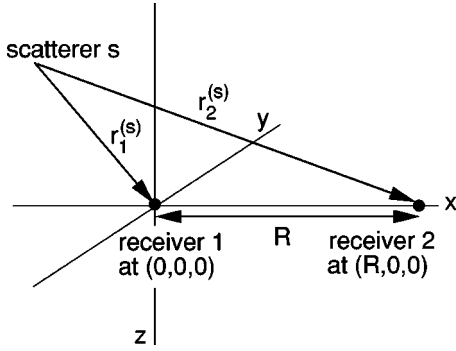


FIG. 1. Definition of the geometric variables for the waves that travel from scatterer number s to two receivers.

$$p_{1,2}(t) = \sum_s S_s \left(t - \frac{r_{1,2}^{(2)}}{c} \right) / r_{1,2}^{(s)}, \quad (1)$$

where c is the wave speed. Because of the directionality of the radiation pattern, the wave forms recorded at the two receivers from a given scatterer are not necessarily equal. As shown later, however, the main contribution to this sum comes from scatterers near the receiver line. The wave traveling from these scatterers to the two receivers propagate in the same direction. Therefore, the directionality of the radiated energy is irrelevant. The constant $-1/4\pi$ in the 3D Green's function is included in the definition of $S_s(t)$. If the response of the receivers depends on frequency, then the impulse response of the receivers can be included in the wave forms $S_s(t)$.

In passive imaging one correlates the waves recorded at two receivers [6] over a time window of length T :

$$C(\tau) \equiv \int_0^T p_2(t+\tau)p_1(t)dt. \quad (2)$$

Inserting Eq. (1) into this expression gives a double sum $\sum_{s,s'}$ over all scatterers

$$C(\tau) = \sum_{s,s'} \int_0^T S_s(t)S_{s'} \left(t + \frac{r_1^{(s')} - r_2^{(s')}}{c} + \tau \right) dt / r_1^{(s')}r_2^{(s')}. \quad (3)$$

Let the autocorrelation of the signal $S_s(t)$ be denoted by

$$C_s(\tau) \equiv \int_0^T S_s(t)S_s(t+\tau)dt. \quad (4)$$

In general, this function is peaked around $\tau=0$. The width of this peak is denoted by Δ , in the jargon of stochastic processes this time is equal to the correlation time of the random process $S_s(t)$. This width may vary among the different signals; if that is the case, Δ indicates the generic width. When the $S_s(t)$ are impulsive functions of time, then Δ is of the same order of magnitude as the width of the $S_s(t)$. When these signals are of a long duration with a quasirandom phase, Δ can be much smaller than the duration of the signals. This property has been successfully employed in radar imaging [19], exploration seismology using vibrators that emit a

quasirandom signal [20], seismic imaging with drill bit noise [21], and time reversed imaging [22].

The double sum $\sum_{s,s'}$ in expression (3) can be split into a sum over diagonal terms $\sum_{s=s'}$ and a sum $\sum_{s \neq s'}$ over cross terms. I show in the Appendix that for a random medium, the ensemble average of the cross terms vanishes provided the dc component of the $S_s(t)$ is equal to zero. In a single realization of the medium, however, the cross terms are nonzero. I also show in the Appendix that for a single source event (e.g. an earthquake) the ratio of the cross terms to the diagonal terms is smaller than $\sqrt{2\Delta/T}$. When an average over N_{src} source events is carried out, this ratio is bounded by $\sqrt{2\Delta/N_{\text{src}}T}$. This means that by averaging over time, and possibly over different source events, the sum of the cross terms can be made arbitrarily small by increasing the time interval T and the number of source events N_{src} . In the following I refer to this type of averaging as *time/event averaging*. Note that in several studies of passive imaging, time/event averaging as described here is the only type of averaging that is applied [5–7,9,10,13].

In the following I assume that sufficient time/event averaging is carried out so that the cross terms in the sum (3) can be ignored. With the definition (4) this reduces expression (3) to

$$C(\tau) = \sum_s C_s \left(\tau + \frac{r_1^{(s)} - r_2^{(s)}}{c} \right) / r_1^{(s)}r_2^{(s)}. \quad (5)$$

Since the Fourier transform of the cross correlation is equal to the power spectrum (5) is given in the frequency domain by

$$C(\omega) = \sum_s |S_s(\omega)|^2 \frac{\exp[i\omega(r_2^{(s)} - r_1^{(s)})/c]}{r_1^{(s)}r_2^{(s)}}. \quad (6)$$

The power spectrum $|S_s(\omega)|^2$ does not depend on the phase fluctuations of the scattered waves, but it does depend on fluctuations in the amplitude. When the variations in the power spectrum are uncorrelated with the phase $\exp[i\omega(r_2^{(s)} - r_1^{(s)})/c]$, then

$$C(\omega) = \overline{|S(\omega)|^2} \sum_s \frac{\exp[i\omega(r_2^{(s)} - r_1^{(s)})/c]}{r_1^{(s)}r_2^{(s)}}, \quad (7)$$

with

$$\overline{|S(\omega)|^2} = \frac{1}{N} \sum_s |S_s(\omega)|^2, \quad (8)$$

where N is the number of scatterers.

When there are many scatterers per wavelength, the summation over scatterers $\sum_s(\dots)$ can be replaced by a volume integration $\int(\dots)ndV$ that is weighted by the scatterer density n that is defined as the number of scatterers per unit volume. In this approximation Eq. (7) is given by

$$C(\omega) = \overline{|S(\omega)|^2} \int \frac{\exp[i\omega(r_2 - r_1)/c]}{r_1 r_2} ndxdydz, \quad (9)$$

with the distances r_1 and r_2 defined in Fig. 2.

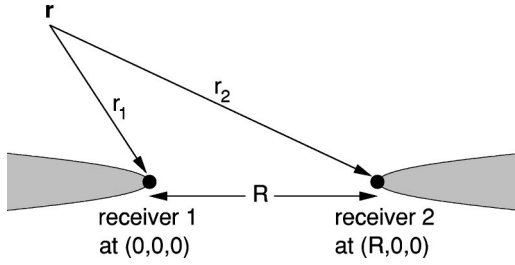


FIG. 2. Definition of the geometric variables for the waves that travel from a scatterer at location \mathbf{r} to two receivers. The region of constructive interference is indicated by the shaded regions.

The integration over the transverse coordinates x and y can be evaluated with the stationary phase approximation [23,24]. This technique leaves only the contribution of the points near the receiver line $y = z = 0$, for which the integrand is not oscillatory. In this approximation

$$C(\omega) = 2\pi \overline{|S(\omega)|^2} \frac{c}{-i\omega} \int_{-\infty}^{\infty} \frac{e^{ik(|R-x|-|x|)}}{|R-x|-|x|} ndx. \quad (10)$$

For scatterers to the left of the receivers ($x < 0$) the integrand is given by $\exp(ikR)/R$, for scatterers to the right of the receivers ($x > R$) the integrand is equal to $\exp(-ikR)/R$, and for scatterers between the receivers ($0 < x < R$) the integrand is given by $\exp(ik(R-2x))/(R-2x)$. Because the latter integrand is oscillatory, the region $0 < x < R$ gives a subdominant contribution to the integral of Eq. (10). Ignoring this contribution gives

$$C(\omega) = 8\pi^2 \overline{|S(\omega)|^2} \left(\frac{c}{i\omega} \right) \times \left(-\frac{e^{ikR}}{4\pi R} \int_{-\infty}^0 ndx - \frac{e^{-ikR}}{4\pi R} \int_R^{\infty} ndx \right). \quad (11)$$

The term $-\exp(ikR)/4\pi R$ is the Green's function that accounts for the waves that propagate between the receivers; this term comes from the integration over $x < 0$. The second term $-\exp(-ikR)/4\pi R$, which comes from the integration over $x > R$, is the advanced Green's function. The retarded Green's function comes from the waves that propagate from receiver 1 to receiver 2 and correlate for a positive lag time $\tau > 0$, as shown in the top panel of Fig. 3. The presence of the advanced Green's function is due to the waves that propagate from receiver 2 to receiver 1; these waves correlate for a negative lag time $\tau < 0$, as shown in the bottom panel of Fig. 3. The factor $1/i\omega$, which corresponds to an integration in the time domain, comes from the stationary phase evaluation of the x and y integrals. In other studies it was also noted that the correlation (2) gives the integral of the sum of the retarded and the advanced Green's functions [6,7,12]. Malcolm *et al.* [8] use this property experimentally as a diagnostic of the equipartitioning of energy.

Each scatterer near the receiver line gives, after time/event averaging, the same contribution to the Green's function. This leads to the integrals $\int_{-\infty}^0 ndx$ and $\int_R^{\infty} ndx$ that

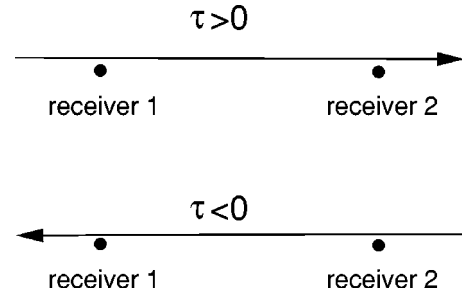


FIG. 3. The waves that propagate toward the right correlate for a positive lag time $\tau > 0$ (top panel), while the waves that are left-moving correlate for a negative lag time $\tau < 0$ (bottom panel).

multiply the retarded and the advanced Green's functions, respectively. If the scatterer density n decreases sufficiently fast toward infinity, these integrals are finite, but in general the integrals are infinite. Furthermore, the scattering losses incurred during the propagation from the scatterers to the receivers have not yet been taken into account. In practice this limits the volume integral to a region of a few mean free paths of the receivers. These unsatisfactory aspects are addressed in the next section.

III. WHICH GREEN'S FUNCTION IS RETRIEVED?

The infinite integrals in Eq. (11) can be removed by considering the physics of passive imaging in more detail. The conclusion of the previous section is that the correlation of the waves recorded at the two receivers yields the Green's function by a process of constructive interference of the scattered waves that propagate along the receiver line. In a scattering medium, the scatterers affect the waves in three ways: (i) the direction of wave propagation is changed by the scatterers, (ii) the velocity of a transmitted wave is affected by scatterers near the path of propagation, and (iii) a transmitted wave attenuates because of scattering losses.

In an ensemble average, the last two effects are described by an effective medium [25,26]. In a single realization of a scattering medium, the scatterers also leave an imprint on the phase velocity and attenuation of a propagating wave. This is illustrated in Fig. 4 which shows the waves that have propagated through a circular region with isotropic point scatterers [27]. The waves in the absence of scatterers are shown with the dashed lines, while the waves in the presence of scatterers are shown by the thin solid lines. All the receivers are at the same distance from the source, yet there are appreciable variations in the amplitude and the phase of the ballistic wave due to the variations in the number of scatterers within the first Fresnel zone for each source-receiver pair. For a given realization and source-receiver pair, a ballistic wave propagates with a phase velocity c , and attenuates over a distance d with a factor $\exp(-d/2L)$. The attenuation length L is not necessarily equal to the mean free path l of the effective medium [25,26] because L is defined for a given path in a single realization.

This principle can be taken into account in Eq. (10) by interpreting c as the phase velocity of the ballistic wave, and

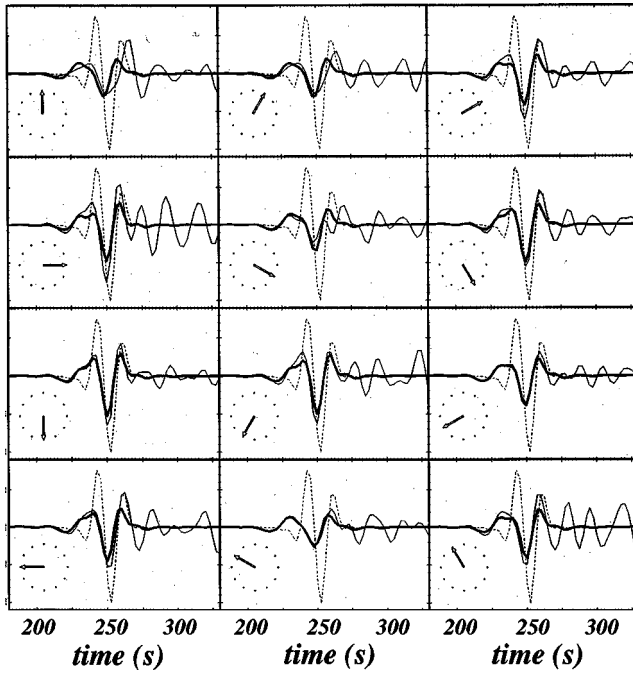


FIG. 4. Waves recorded at twelve locations at the edge of a circular region that contains isotropic point scatterers [27]. The clock indicates the receiver position. Shown is the wave field in the absence of scatterers (dashed line), the complete wave field in the presence of scatterers (thin solid line), and the wave field computed by averaging the scatterers within the first Fresnel zone for each receiver (thick solid line).

by multiplying the integrand with a factor $\exp[-(|R-x|+|x|)/2L]$ that accounts for the scattering losses of the waves that travel to both receivers. For a constant scatterer density n , the x integrals that correspond to those in Eq. (10) can be carried out to give

$$C(\omega) = 8\pi^2 \overline{|S(\omega)|^2} \left(\frac{ncL}{i\omega} \right) \left(-\frac{e^{ikR}e^{-R/2L}}{4\pi R} - \frac{e^{-ikR}e^{-R/2L}}{4\pi R} \right). \quad (12)$$

The x integrals contribute a factor L to the correlation. The last two terms give the retarded and advanced Green's functions for the ballistic wave that propagates between the receivers.

The issue of the medium of propagation is also of relevance for the derivation of passive imaging based on normal modes [6]. That derivation has an open question: the normal modes of which system should be used? The normal modes of the true system, which includes the scatterers, are by definition uncoupled; equipartitioning among these modes therefore will not occur. The normal modes of a homogeneous system are coupled by the scatterers, which may result in equipartitioning of energy among the modes of the homogeneous model. However, this raises the question which homogeneous system to use? It is not clear from the derivation of Lobkis and Weaver [6] from which system one obtains the Green's function. If this would be the Green's function of a medium that takes the scattering losses of the ballistic wave into account, then that medium is attenuating. In such a me-

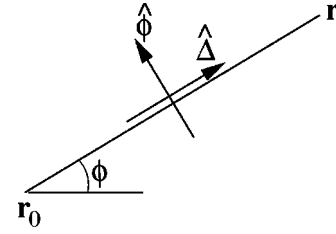


FIG. 5. Definition of the unit vectors $\hat{\Delta}$ and $\hat{\phi}$ that define the radial and transverse polarizations, respectively.

diuum the normal modes are not orthogonal and the theory of Lobkis and Weaver [6] must be generalized by using adjoint modes [28].

IV. SURFACE WAVES IN AN ELASTIC MEDIUM

Campillo and Paul [6] obtained the full surface wave Green's tensor by correlating the direct product of the three components of the two receivers. In this section, I show that the treatment of the previous sections can be generalized to surface waves propagating in a layered elastic 3D medium with embedded scatterers. The surface-wave Green's tensor of a layered medium whose properties depend on the depth z only can be written in the frequency domain as

$$G_{ij}(\mathbf{r}, \mathbf{r}_0) = \sum_m G_{ij}^m(\mathbf{r}, \mathbf{r}_0). \quad (13)$$

The total surface wave Green's tensor is expressed as a sum over surface-wave modes m that include both Rayleigh waves and Love waves. The surface wave Green's tensor of mode m in the far field is given by [29,30]

$$G_{ij}^m(\mathbf{r}, \mathbf{r}_0) = p_i^m(z, \varphi) p_j^{m*}(z_0, \varphi) \frac{e^{i(k_m R + \pi/4)}}{\sqrt{\frac{\pi}{2} k_m R}}, \quad (14)$$

where $R = \sqrt{(x-x_0)^2 + (y-y_0)^2}$ is the distance between the points measured in the horizontal plane, and k_m is the horizontal wave number of mode m . The polarization vectors $\mathbf{p}^m(z, \varphi)$ depend on the depth z and the azimuth φ of the path between points \mathbf{r}_0 and \mathbf{r} . The orientation of the polarization vectors can be expressed into the unit vectors $\hat{\Delta}$ and $\hat{\phi}$ that point in the radial and transverse direction, respectively, as defined in Fig. 5. For Love waves the polarization vector is related to the Love wave eigenfunction $l_1^m(z)$ [29,31] by

$$\mathbf{p}^m(z, \varphi) = l_1^m(z) \hat{\phi}, \quad (15)$$

while for Rayleigh waves

$$\mathbf{p}^m(z, \varphi) = r_1^m(z) \hat{\Delta} + i r_2^m(z) \hat{\mathbf{z}}, \quad (16)$$

with $r_1^m(z)$ and $r_2^m(z)$ the radial- and vertical-component modal functions of the Rayleigh waves [29,31]. Following Ref. [29], the surface-wave modes are assumed to be normalized according to the following convention:

$$4c_m U_m \int_0^\infty \rho(l_1^m)^2 dz = 4c_m U_m \int_0^\infty \rho[(r_1^m)^2 + (r_2^m)^2] dz = 1, \quad (17)$$

with c_m and U_m are the phase velocity and group velocity of mode m , respectively, and $\rho(z)$ the mass density.

When the two receivers record the three components of the ground motion, one can form the correlation tensor of all combinations of components

$$C_{ij}(\tau) = \int u_{2i}(t+\tau)u_{1j}(t)dt, \quad (18)$$

where u_{2i} , for example, is the i component of the displacement recorded at receiver 2. The recorded displacement can be written as a sum over the surface waves radiated by the different scatterers s . By analogy with Eq. (1) the displacement of the two receivers in the frequency domain is given by a double sum over scatterers s and surface wave modes m

$$\mathbf{u}_{1,2} = \sum_s \sum_m \mathbf{p}^m(z_{1,2}, \varphi_{1,2}^{(s)}) \frac{e^{i(k_m X_{1,2}^{(s)} + \pi/4)}}{\sqrt{k_m X_{1,2}^{(s)}}} S^{(s,m)}(\omega). \quad (19)$$

In this expression $X_{1,2}^{(s)}$ is the horizontal distance between scatterer s and receiver 1 and 2, respectively, $\varphi_{1,2}^{(s)}$ is the azimuth of the corresponding scattering path, and $S^{(s,m)}(\omega)$ is the frequency spectrum of the radiation of mode m from scatterer s . Inserting this expression in the correlation (18) gives a double sum $\sum_{s,s'}$ over scatterers. The cross terms $s \neq s'$ interfere after sufficient time/event averaging destructively and can be ignored. The resulting sum $\sum_s(\dots)$ can be approximated with the surface integral $\int(\dots)n dx dy$, where n is the scatterer density per unit surface area. Taking these steps gives

$$C_{ij}(\omega) = \sum_{m,m'} \int dx dy n p_i^m(z_2, \varphi_2) p_j^{m'*}(z_1, \varphi_1) \times \frac{e^{i(k_m X_2 - k_{m'} X_1)}}{\sqrt{k_m k_{m'} X_2 X_1}} S^m(\omega) S^{m'*}(\omega), \quad (20)$$

where it is understood that all quantities in Eq. (19) that depend on the scatterer s now depend on the location (x,y) of the integration point.

The integral over the transverse coordinate y can be evaluated in the stationary phase approximation, this gives a contribution from scatterers near the receiver line that is given by

$$C_{ij}(\omega) = \sqrt{2\pi} \sum_{m,m'} \int dx n p_i^m(z_2, \pm) p_j^{m'*}(z_1, \pm) \times \frac{e^{i(k_m |x-R| - k_{m'} |x|)} e^{i\eta\pi/4}}{\sqrt{k_m k_{m'} \sqrt{|k_m |x| - k_{m'} |x-R|}}} S^m(\omega) S^{m'*}(\omega), \quad (21)$$

with

$$\eta \equiv \begin{cases} +1 & \text{if } \frac{k_m}{|x-R|} - \frac{k_{m'}}{|x|} > 0, \\ -1 & \text{if } \frac{k_m}{|x-R|} - \frac{k_{m'}}{|x|} < 0. \end{cases} \quad (22)$$

The azimuth associated with the polarization vectors in Eq. (21) is given by $\varphi=0$ for $x<0$ and by $\varphi=\pi$ for $x>R$; these cases are denoted by the plus and minus sign, respectively.

The integrand of Eq. (21) is oscillatory, except when $k_m = k_{m'}$. This means that the dominant contribution comes from the terms $m=m'$, for this reason the mode coupling terms $m \neq m'$ can be ignored. Furthermore, the integrand is oscillatory over the range $0 < x < R$, and the dominant contribution comes from the regions $x < 0$ and $x > R$. These approximations give

$$C_{ij}(\omega) = \pi \sum_m \left\{ \frac{1}{ik_m} \int_{-\infty}^0 dx n p_i^m(z_2, +) p_j^{m'*}(z_1, +) \times \frac{e^{i(k_m R + \pi/4)}}{\sqrt{\frac{\pi}{2} k_m R}} - \frac{1}{ik_m} \int_R^\infty dx n p_i^m(z_2, -) \times p_j^{m'*}(z_1, -) \frac{e^{-i(k_m R + \pi/4)}}{\sqrt{\frac{\pi}{2} k_m R}} \right\} \overline{|S^m(\omega)|^2}, \quad (23)$$

with $\overline{|S^m(\omega)|^2}$ the average power spectrum of the radiated mode m . The first term is due to right-going waves that are generated in the region $x < 0$, the polarization vectors correspond to the azimuth $\varphi=0$, which is indicated by the plus signs. The second term is due to waves scattered from the area $x > R$ that move toward the left, their polarization vectors correspond to the azimuth $\varphi=\pi$, which is indicated by the minus signs.

Note that the stationary phase integration over the transverse coordinate leads to the correct geometrical spreading $1/\sqrt{k_m R}$. When the (secondary) sources of the waves are confined to the vertical plane through the source and receiver, the integral over the transverse coordinate is absent. This is the reason why the geometrical spreading is not correctly retrieved in the derivation of Roux and Fink [11].

A comparison with Eq. (14) shows that the first term is equal to $(c_m/i\omega)G_{ij}^m(\mathbf{r}_2, \mathbf{r}_1)$, while the second one equals $[(c_m/i\omega)G_{ji}^m(\mathbf{r}_1, \mathbf{r}_2)]^*$. The correlation tensor is therefore given by

$$C_{ij}(\omega) = \pi \sum_m c_m \left\{ \frac{G_{ij}^m(\mathbf{r}_2, \mathbf{r}_1)}{i\omega} \int_{-\infty}^0 dx n + \left(\frac{G_{ji}^m(\mathbf{r}_1, \mathbf{r}_2)}{i\omega} \right)^\dagger \int_R^\infty dx n \right\} \overline{|S^m(\omega)|^2}, \quad (24)$$

where the dagger denotes the Hermitian conjugate. This expression contains infinite integrals. Incorporating the attenuative properties of the ballistic surface wave, as shown in Sec. III, gives

$$C_{ij}(\omega) = \pi \sum_m \overline{|S^m(\omega)|^2} n c_m L_m \times \left\{ \frac{G_{ij}^m(\mathbf{r}_2, \mathbf{r}_1)}{i\omega} + \left(\frac{G_{ij}^m(\mathbf{r}_1, \mathbf{r}_2)}{i\omega} \right)^\dagger \right\}, \quad (25)$$

where L_m is attenuation length of surface wave mode m , and where the Green's function of each mode is understood to contain an attenuation term $\exp(-R/2L_m)$.

This expression is similar to the corresponding result (12) for scalar waves in three dimensions. The correlation gives the superposition of the Green's function of the ballistic wave that propagates from receiver 1 to receiver 2 (the first term), and the ballistic wave Green's function that propagates in the opposite direction (the last term). Passive imaging with surface waves thus provides the superposition of the retarded and advanced surface wave Green's functions of the ballistic wave.

V. CONCLUSION

As shown in Eqs. (11) and (25), the ballistic wave Green's function can be obtained by a cross correlation of the wave forms at two receivers. Two steps must be taken to extract this Green's function from the correlation. First, the correlation in the frequency domain must be multiplied by $i\omega/\overline{|S(\omega)|^2}$. The multiplication with $i\omega$ corresponds in the time domain to a differentiation that undoes the integration used in the cross correlation. The division by the power spectrum $\overline{|S(\omega)|^2}$ corrects for frequency-dependent factors in the scattering coefficients, the source spectrum, and the receiver response. For the case of Eq. (11) for scalar waves in 3D, the power spectrum can be obtained from the waves recorded at the receivers. For the corresponding expression (25) for surface waves in an elastic medium, each mode must be corrected for the power spectrum of that mode. The scattering coefficients for surface wave modes strongly depend on the depth of the scatterers [29], and on topography [32]. For this reason the average power spectrum $\overline{|S^m(\omega)|^2}$ of the scattered surface wave mode may depend strongly on the mode number m . It is not clear how $\overline{|S^m(\omega)|^2}$ can be extracted from the recorded waves. In applications in crustal seismology, the fundamental mode Love and Rayleigh waves usually dominate. The average power in the fundamental Rayleigh wave can be estimated from the vertical component. The power of the horizontal components can then be used to infer the power in the fundamental Love wave. Without correcting for the power spectrum, the cross correlation may not give the correct frequency dependence of the Green's function.

The second step that must be taken is due to the fact that the cross correlation of the waves recorded at two receivers gives the superposition of the retarded and the advanced ballistic wave Green's functions. These two contributions can be unraveled in the time domain by restricting the signal to

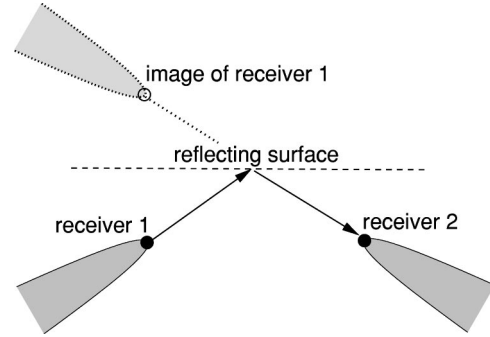


FIG. 6. The wave path of a reflected wave. The receivers are shown by solid circles. The dark gray areas indicate the location of scatterers that give a stationary contribution to the integration over scatterers for the reflected wave. The open circle denotes the image of receiver 1 upon reflection in the free surface, and the light gray area is the image of the scatterers that contribute to the stationary phase solution for the reflected wave.

positive and negative time windows, respectively [6].

Physically, the derivation shown here implies that in general the scattered waves recorded at the two receivers are uncorrelated, except for the waves radiated from scatterers that are located near the receiver line. Passive imaging of the ballistic wave thus is based on constructive interference solely of those scattered waves that propagate along the receiver line.

Ultrasound experiments with a finite aluminum sample show that the ballistic wave as well as waves that are reflected from boundaries are reconstructed from passive imaging [6,9,10]. The theory presented here does not account for these reflected waves. When a wave reflects off a plane boundary, as shown in Fig. 6, the scattering paths from scatterers located in the dark gray areas interfere constructively. The theory presented here can be applied to this problem by invoking an image receiver and image scatterers as indicated by the open circle and light-gray area in Fig. 6. For a non-planar boundary or an inhomogeneous reference medium one needs to determine other stationary phase contributions to the integral over the scatterers. These contributions depend on the geometry of scattering path, and are not accounted for by the theory presented here.

The equilibration of normal modes [6] provides a sufficient condition for constructing the Green's function from the cross correlation of the waves recorded at two receivers. The derivation presented here shows, however, that the equilibration of normal modes is not a necessary condition. In fact, the derivation presented here is equally valid for open systems that do not possess normal modes. The derivation also holds for closed systems that do possess normal modes at early times when the modes have not yet equilibrated.

The derivation presented here is based on the assumption that the scattered waves propagate isotropically in all directions. (This does not imply that the scattering coefficients are isotropic; it means that the net energy flux of the scattered waves is small.) Mathematically this is expressed by the condition that the scatterer density n is constant in space. This implies a local condition on the isotropic propagation of scat-

tered waves near the receivers, rather than the global requirement of the equilibration of normal modes. By using the correlations that are hidden in the coda waves, the destructive interference of waves radiated from scatterers away from the receiver line, and the constructive interference of scattered waves that propagate along the receiver line makes passive imaging an effective technique for extracting the ballistic wave Green's function between two points without using a source at either of these points.

ACKNOWLEDGMENTS

I am much indebted to Arnaud Derode who reviewed an earlier version of this manuscript—his critical and constructive input has been crucial. I also appreciate the comments from and discussions with Ken Lerner, Matt Haney, John Scales, and Alison Malcolm. This work was supported by the NSF (Grant No. EAR-0106668) and by the sponsors of the Consortium Project on Seismic Inverse Methods for Complex Structures at the Center for Wave Phenomena.

APPENDIX: ESTIMATION OF THE CROSS TERMS IN A SINGLE REALIZATION

Since the scattered waves in a complex medium have a random character, I estimate the cross terms $\sum_{s \neq s'}$ in the sum (3) for a random medium. In this model, the scatters are randomly located in the medium and the location of different scatterers is uncorrelated. In the following, I assume that the dc component of the signals vanishes. If this is the case, then

$$\langle S_s(t) \rangle = 0. \quad (\text{A1})$$

In this appendix the angled brackets $\langle \dots \rangle$ indicate an ensemble average. It is essential that the dc component of the scattered waves vanish; when the dc component is nonzero there is no destructive interference, and averaging over the scatterer positions does not give a vanishing mean signal.

The waves emitted by scatters s and s' are in the ensemble average uncorrelated because the position of these scatterers are uncorrelated. This means that

$$\langle S_s(t) S_{s'}(t') \rangle = \langle S_s(t) \rangle \langle S_{s'}(t') \rangle = 0 \quad \text{for } s \neq s', \quad (\text{A2})$$

where expression (A1) is used in the last identity. Following the notation of expression (4) we have for the diagonal terms

$$\langle S_s(t) S_s(t') \rangle = C_s(t-t'). \quad (\text{A3})$$

Strictly speaking this covariance may depend on the time t as well, because the time series $S_s(t)$ is not necessarily stationary. This can be incorporated by replacing expression (A3) by $\langle S_s(t) S_s(t') \rangle = W(t) C_s(t-t')$, where $W(t)$ varies slowly with time compared to $C_s(t-t')$ and compared to the width of the employed time window. This complication can be incorporated by replacing $C_s(t-t')$ by $W(t) C_s(t-t')$. Since this does not change the essence of the argument, this is not included in the following.

Let us consider the sum (3) and ignore for the moment the geometrical spreading terms $r_1^{(s)} r_2^{(s)}$. These terms can be in-

serted at the end, but they do not change the essence of the argument. Absorbing the term $(r_1^{(s)} - r_2^{(s)})/c$ into τ , expression (3) becomes

$$C(\tau) = \underbrace{\sum_s \int_0^T S_s(t) S_s(t+\tau) dt}_{C_D(\tau)} + \underbrace{\sum_{s \neq s'} \int_0^T S_s(t) S_{s'}(t+\tau) dt}_{C_C(\tau)}, \quad (\text{A4})$$

where the first term denotes the diagonal term $C_D(\tau)$ and the second term gives the cross term $C_C(\tau)$. Because of Eq. (A2) the expectation value of the cross term vanishes:

$$\langle C_C(\tau) \rangle = \sum_{s \neq s'} \int_0^T \int_0^T \langle S_s(t) S_{s'}(t+\tau) \rangle dt = 0. \quad (\text{A5})$$

In a single realization, however, the cross term $C_C(\tau)$ is in general nonzero. I estimate its value by analyzing the variance $\langle C_C^2(\tau) \rangle$. Using expression (A4) this variance is given by

$$\langle C_C^2(\tau) \rangle = \sum_{s \neq s', u \neq u'} \int_0^T \int_0^T \langle S_s(t) S_u(t') S_{s'}(t+\tau) \times S_{u'}(t'+\tau) \rangle dt dt'. \quad (\text{A6})$$

Since the different $S_s(t)$ are uncorrelated [expression (A2)], the only terms that give a nonzero contribution to Eq. (A6) are the terms $s=u$ and $s'=u'$ or the terms $s=u'$ and $s'=u$. This gives

$$\langle C_C^2(\tau) \rangle = \sum_{s \neq s'} \int_0^T \int_0^T \{ \langle S_s(t) S_s(t') \rangle \langle S_{s'}(t+\tau) S_{s'}(t'+\tau) \rangle + \langle S_s(t) S_{s'}(t'+\tau) \rangle \langle S_{s'}(t') S_s(t+\tau) \rangle \} dt dt'. \quad (\text{A7})$$

With the definition (A3) this can be written as

$$\langle C_C^2(\tau) \rangle = \sum_{s \neq s'} \int_0^T \int_0^T \{ C_s(t-t') C_{s'}(t-t') + C_s(t-t'-\tau) C_{s'}(t-t'+\tau) \} dt dt'. \quad (\text{A8})$$

Now let us estimate the order of magnitude of this sum. When there are N scatterers contributing to this sum, then there are $N(N-1) < N^2$ terms in the double sum. Let the maximum of $C_s(t)$ be given by C_{\max} . This maximum may be different for the different $C_s(t)$, if that is the case then C_{\max} is the largest of all these maxima. The width of the autocorrelation $C_s(t)$ is indicated by Δ . Each of the t' integrals in Eq. (A8) then gives a contribution that is smaller than $C_{\max}^2 \Delta$. The remaining t integral gives a contribution T . This implies that

$$\langle C_C^2(\tau) \rangle \leq 2N^2 C_{\max}^2 T \Delta. \quad (\text{A9})$$

In order to assess the importance of the cross terms, I compare this with the mean of the diagonal term. This mean is given by

$$\langle C_D(0) \rangle = \sum_s \int_0^T \langle S_s^2(t) \rangle dt = \sum_s \int_0^T \langle C_s(0) \rangle dt. \quad (\text{A10})$$

Using the same estimates that led to Eq. (A9) then gives

$$\langle C_D(0) \rangle = \sum_s C_s(0) T \approx N C_{\max} T, \quad (\text{A11})$$

because the autocorrelation attains its maximum for a zero time lag. With the estimate (A9) this gives the following ratio of the standard deviation of the cross terms to the diagonal terms:

$$\frac{\langle C_C^2(\tau) \rangle^{1/2}}{\langle C_D(0) \rangle} \leq \sqrt{\frac{2\Delta}{T}}. \quad (\text{A12})$$

Note that this ratio does not depend on the number of scatterers. When in addition to an averaging over time, N_{src} source events are used, and when the signals emitted by the scatterers for different source events are uncorrelated, the standard deviation of the cross terms increases with a factor $\sqrt{N_{\text{src}}}$ while the diagonal terms are proportional to N_{src} , so that

$$\frac{\langle C_C^2(\tau) \rangle^{1/2}}{\langle C_D(0) \rangle} \leq \sqrt{\frac{2\Delta}{N_{\text{src}} T}}. \quad (\text{A13})$$

-
- [1] R. Snieder, A. Grêt, H. Douma, and J. Scales, *Science* **295**, 2253 (2002).
- [2] M. L. Cowan, I. P. Jones, J. H. Page, and D. A. Weitz, *Phys. Rev. E* **65**, 066605 (2002).
- [3] J. N. Louie, *Bull. Seismol. Soc. Am.* **91**, 347 (2001).
- [4] K. Wapenaar, D. Draganov, J. Thorbecke, and J. Fokkema, *Geophys. J. Int.* **156**, 179 (2004).
- [5] J. E. Rickett and J. F. Claerbout, *Sol. Phys.* **192**, 203 (2000).
- [6] O. I. Lobkis and R. L. Weaver, *J. Acoust. Soc. Am.* **110**, 3011 (2001).
- [7] A. Derode, E. Larose, M. Campillo, and M. Fink, *Appl. Phys. Lett.* **83**, 3054 (2003).
- [8] A. Malcolm, J. A. Scales, and B. van Tiggelen (unpublished).
- [9] R. L. Weaver and O. I. Lobkis, *Phys. Rev. Lett.* **87**, 134301 (2001).
- [10] R. Weaver and O. Lobkis, *Ultrasonics* **40**, 435 (2003).
- [11] P. Roux and M. Fink, *J. Acoust. Soc. Am.* **113**, 1406 (2003).
- [12] A. Derode, E. Larose, M. Tanter, J. de Rosny, A. Tourin, M. Campillo, and M. Fink, *J. Acoust. Soc. Am.* **113**, 2973 (2003).
- [13] M. Campillo and A. Paul, *Science* **299**, 547 (2003).
- [14] S. Stein and M. Wyssession, *An Introduction to Seismology, Earthquakes, and Earth Structure* (Blackwell, Malden, MA, 2003).
- [15] H. Takeuchi and M. Saito, in *Seismology: Surface Waves and Earth Oscillations, Vol. II of Methods in Computational Physics*, edited by B. A. Bolt (Academic Press, New York, 1972).
- [16] F. A. Dahlen and J. Tromp, *Theoretical Global Seismology* (Princeton University Press, Princeton, 1998).
- [17] T. Tanimoto, *Geophys. J. R. Astron. Soc.* **89**, 713 (1987).
- [18] B. Romanowicz, in *International Handbook of Earthquake and Engineering Seismology*, edited by W. H. K. Lee, H. Kanamori, P. C. Jennings, and C. Kisslinger (Academic Press, New York, 2003), pp. 149–173, Pt. B.
- [19] J. P. Nathanson, F. E. znd Reilly, and M. N. Cohen, *Radar Design Principles*, 2nd ed. (Scitech Publishing, Mendham, 1999).
- [20] P. L. Goupillaud, *Geophysics* **41**, 1291 (1976).
- [21] J. W. Rector and B. P. Marion, *Geophysics* **56**, 628 (1991).
- [22] A. Derode, A. Tourin, and M. Fink, *J. Appl. Phys.* **85**, 6343 (1999).
- [23] C. M. Bender and S. A. Orszag, *Advanced Mathematical Methods for Scientists and Engineers* (McGraw-Hill, New York, 1978).
- [24] N. Bleistein, *Mathematical Methods for Wave Phenomena* (Academic Press, Orlando, 1984).
- [25] U. Frisch, in *Probabilistic Methods in Applied Mathematics*, edited by A. T. Bharucha-Reid (Academic Press, New York, 1968), pp. 75–198.
- [26] P. Sheng, *Introduction to Wave Scattering, Localization, and Mesoscopic Phenomena* (Academic Press, San Diego, 1995).
- [27] J. Groenenboom and R. Snieder, *J. Acoust. Soc. Am.* **98**, 3482 (1995).
- [28] J. Park and F. Gilbert, *J. Geophys. Res.* **91**, 7241 (1986).
- [29] R. Snieder, *Geophys. J. R. Astron. Soc.* **84**, 581 (1986).
- [30] R. Snieder, in *Scattering and Inverse Scattering in Pure and Applied Science*, edited by R. Pike and P. C. Sabatier (Academic Press, San Diego, 2002), Chap. 1.7.3, pp. 562–577.
- [31] K. Aki and P. G. Richards, *Quantitative Seismology*, 2nd ed. (University Science Books, Sausalito, 2002).
- [32] R. Snieder, *Phys. Earth Planet. Inter.* **44**, 226 (1986).